Discrete wave-packet representation in nuclear matter calculations

H. Müther*
Institute for Theoretical Physics, University of Tübingen, Auf der Morgenstelle 14, D-72076 Tübingen, Germany

O. A. Rubtsova,† V. I. Kukulin,‡ and V. N. Pomerantsev§
Skobeltsyn Institute of Nuclear Physics, Moscow State University, Leninskie gory 1(2), Moscow, 119991, Russia
(Received 27 June 2016; published 19 August 2016)

The Lippmann-Schwinger equation for the nucleon-nucleon t matrix as well as the corresponding Bethe-Goldstone equation to determine the Brueckner reaction matrix in nuclear matter are reformulated in terms of the resolvents for the total two-nucleon Hamiltonians defined in free space and in medium correspondingly. This allows one to find solutions at many energies simultaneously by using the respective Hamiltonian matrix diagonalization in the stationary wave-packet basis. Among other important advantages, this approach simplifies greatly the whole computation procedures both for the coupled-channel t matrix and the Brueckner reaction matrix. Therefore this principally novel scheme is expected to be especially useful for self-consistent nuclear matter calculations because it allows one to accelerate in a high degree single-particle potential iterations. Furthermore the method provides direct access to the properties of possible two-nucleon bound states in the nuclear medium. The comparison between reaction matrices found via the numerical solution of the Bethe-Goldstone integral equation and the straightforward Hamiltonian diagonalization shows a high accuracy of the method suggested. The proposed fully discrete approach opens a new way to an accurate treatment of two- and three-particle correlations in nuclear matter on the basis of the three-particle Bethe-Faddeev equation by an effective Hamiltonian diagonalization procedure.

DOI: 10.1103/PhysRevC.94.024328

I. INTRODUCTION

The conventional treatment of quantum problems with continuous spectrum (e.g., few-body scattering problems) uses either the differential Schroedinger-type equation with the appropriate boundary conditions or employs an integral equation of the Lippmann-Schwinger or Faddeev type [1]. A somewhat similar formalism is used in the nuclear matter calculations within the Brueckner-Bethe-Goldstone approach [2–7] for finding the Brueckner reaction matrix to treat strong two- or few-particle correlations in the many-nucleon system.

However, there are alternative approaches in quantum scattering which allow one to evaluate scattering observables as well as the fully off-shell transition operator by using some spectral properties of the Hamiltonian. In this alternative way, one employs a finite-dimensional approximation for the spectral expansion of the total resolvent within the continuum discretization technique [8] or uses another L_2-type approach [9–12]. By using this approximation, the initial Lippmann-Schwinger equation for the scattering t matrix is rewritten in a form which includes the total resolvent expressed as a finite sum over the total Hamiltonian bound and pseudostates. Thus, a single Hamiltonian matrix diagonalization makes it possible to determine scattering observables for all necessary energies in a very broad interval. This discrete way for solving a single-channel scattering problem becomes even more efficient in a coupled-channel case because it results in getting the multichannel off-shell t matrix at many energies simultaneously.

Keeping in mind that the Bethe-Goldstone equation (BGE) for the reaction matrix in nuclear matter differs from the Lippmann-Schwinger equation (LSE) by the presence of the Pauli-projection operator in its kernel, one can try to replace the solution of the BGE also with a straightforward diagonalization procedure of the respective Hamiltonian matrix calculated on the appropriate basis.

The specific feature of the nuclear matter calculations is that one has to solve the respective integral BGE many times to obtain the reaction matrix for the various values of relative and center-of-mass momenta and energies needed to evaluate, e.g., the single-particle potential in a derivation of the equation of state (EOS) [2,3]. We keep in mind that one employs usually an iterative procedure to calculate the single-particle potential in a self-consistent way. Thus, to find the EOS one has to carry out quite a few iteration steps to attain a self-consistent solution for solving the Bethe-Goldstone integral equation at many energies [3]. These self-consistent iterations are time-consuming but still feasible on modern computer systems. The numerical efforts, however, increase considerably if one tries to account for an accurate treatment of three-body correlations in nuclear matter using two- and three-body forces on the basis of the Bethe-Faddeev equations [7]. Therefore it is highly desirable to develop efficient tools for the solution of these equations.

Thus, in the present paper we employ the wave-packet continuum discretization technique [8] to carry out single- and coupled-channel scattering calculations with realistic NN interaction in vacuum as well as in medium by using

*herbert.muether@uni-tuebingen.de
†rubtsova@nucl-th.sinp.msu.ru
‡kukulin@nucl-th.sinp.msu.ru
§pomeran@nucl-th.sinp.msu.ru

finite-dimensional approximation for the total resolvent. This technique leads to an efficient way of solving the two-nucleon (NN) problem with continuous single-particle spectra. In addition, this method will also give explicit access to the properties of the bound and quasibound states of two nucleons in vacuum as well as in infinite matter (see, e.g., the discussion of possible di-neutron states in neutron matter [13] and references cited there).

The structure of the paper is the following: In Sec. II, we explain in detail our approach to finding the fully off-shell t matrix at many energies simultaneously via a direct diagonalization of the total Hamiltonian matrix by using the basis of stationary wave packets. Further, in Sec. III, this approach is generalized to the solution for the Bethe-Goldstone equation in nuclear matter. This alternative way turned out to be simpler and faster as compared to the conventional approach as is demonstrated in Sec. IV which contains some illustrative examples. This section also includes a discussion of bound two-nucleon states in the medium of nuclear matter. The summary is given in Sec. V. For the reader's convenience we have added the Appendix with some details of the discrete coupled-channel formalism.

II. SINGLE- AND COUPLED-CHANNEL SCATTERING PROBLEM IN A DISCRETE REPRESENTATION

A. t matrix for a two-body scattering problem

Let us start with remembering some well-known formulas from the quantum scattering theory [1]. The integral Lippmann-Schwinger equation for the transition operator in momentum representation (t matrix) corresponding to a scattering of two particles with momenta $\mathbf{k}_1$ and $\mathbf{k}_2$ has the following form:

$$t(\mathbf{k},\mathbf{k}';E) = V(\mathbf{k},\mathbf{k}') + \int \frac{d^3k'' V(\mathbf{k},\mathbf{k}'')t(\mathbf{k}'',\mathbf{k}';E)}{E + \mathrm{i}0 - \frac{(k'')^2}{2\mu}}, \quad (1)$$

where $\mathbf{k} = \mathbf{k}_2 - \mathbf{k}_1$ (and also $\mathbf{k}'$, $\mathbf{k}''$) is the relative momentum of the particles, V is an interaction potential, μ is the reduced mass, and the center of mass momentum dependence is assumed to be separated out.

In operator form, Eq. (1) is written,

$$\hat{t}(E) = \hat{V} + \hat{V}\hat{g}_0(E)\hat{t}(E), \quad (2)$$

where $\hat{g}_0(E) = [E + i0 - \hat{h}_0]^{-1}$ is the resolvent of the free Hamiltonian $\hat{h}_0$ (the kinetic energy operator) or the Greens function for the noninteracting particles.

Alternatively one can introduce the resolvent $\hat{g}(E) = [E + i0 - \hat{h}]^{-1}$ of the total Hamiltonian $\hat{h} = \hat{h}_0 + \hat{V}$ including the interaction. This total resolvent is related to the free resolvent $\hat{g}_0(E)$ by the well-known identity:

$$\hat{g}(E) = \hat{g}_0(E) + \hat{g}_0(E)\hat{V}\hat{g}(E). \quad (3)$$

If one knows the total resolvent $\hat{g}(E)$, the transition operator (2) can be evaluated straightforwardly from the relation:

$$\hat{t}(E) = \hat{V} + \hat{V}\hat{g}(E)\hat{V}. \quad (4)$$

At first glance the evaluation of the total resolvent from the integral Eq. (3) seems to be a more complicated task than the calculation of the half-shell t matrix through the integral equation (2) at a single fixed energy. However, there are some L_2 techniques [8–12] which allow one to find a finite-dimensional approximation for $\hat{g}(E)$ and calculate the t-matrix elements directly using the relation (4).

These finite-dimensional approximations are usually based on a spectral expansion of the total resolvent using a complete set of states for the total Hamiltonian $\hat{h}$, i.e., using its bound $\{|\psi_n^\alpha\rangle\}$ and continuum states $\{|\psi^\alpha(E)\rangle\}$:

$$\hat{g}(E) = \sum_\alpha \sum_n \frac{|\psi_n^\alpha\rangle\langle\psi_n^\alpha|}{E - E_n} + \sum_\alpha \int_0^\infty dE' \frac{|\psi^\alpha(E')\rangle\langle\psi^\alpha(E')|}{E + \mathrm{i}0 - E'}, \quad (5)$$

where α are appropriate quantum numbers referring to operators which commute with the Hamiltonian. Approximating the spectral expansion (5) by a finite sum over the Hamiltonian $\hat{h}$ pseudostates $\{|z_k^\alpha\rangle\}$ found in some appropriate L_2 basis [8,9], one gets the following finite-dimensional form for the total resolvent $g(E)$:

$$\hat{g}(E) \approx \sum_\alpha \sum_n \frac{|\psi_n^\alpha\rangle\langle\psi_n^\alpha|}{E - E_n} + \sum_{\alpha,k} |z_k^\alpha\rangle g_k^\alpha(E)\langle z_k^\alpha|. \quad (6)$$

Here $g_k^\alpha(E)$ are complex functions which depend on energy E and pseudostate energies $\{E_k^\alpha\}$ only. So this expansion allows one to find the resolvent $\hat{g}(E)$ and, furthermore, the off-shell t matrix at any energy E by using only *a single diagonalization of the total Hamiltonian matrix* for each channel α [only functions $g_k^\alpha(E)$ should be recalculated which is straightforward].

It should be mentioned that this "spectral" scheme is very convenient because it allows one to use any complete system of eigenstates of the total Hamiltonian, such as standing wave scattering functions [1] which are real valued. In other words, the spectral expansion does not require an accurate treatment of boundary conditions for states in the numerator of (5) (that is why the pseudostates can successfully be used here). Below, we use for this purpose the method of the wave-packet continuum discretization (WPCD) developed by the present authors in previous years [8]. This general approach was demonstrated [8,14] to be fully applicable for a coupled-channel interaction case as well (see also the Appendix to the present paper).

One of the main purposes of this paper is a careful testing of the diagonalization procedure for construction of the coupled-channel t matrix for some realistic cases and also the generalization of such a diagonalization approach to the solution of the Bethe-Goldstone–type equation widely used in nuclear matter calculations. So below we discuss the case of NN scattering with the realistic interaction including strong tensor components which results in coupled-channel equations. However, the scheme discussed is applicable also for other types of coupled-channel problems, e.g., arising in a coupled-channel reduction for some few-body scattering problems [15].

B. Solution of a coupled-channel Lippmann-Schwinger equation in a wave-packet representation

In this development, we apply a partial-wave expansion for antisymmetrized wave functions and operators over the plane wave states $|k\rangle$ with definite orbital momentum l, spin s, and total angular momentum j for the interacting nucleons (the isospin value τ is determined by the l and s values, so we omit it here to simplify notations).

Then, after the partial-wave projection, the integral LSE (1) takes the following form for given values of j and s (those are conserved for the NN Hamiltonian):

$$t^{js}_{ll'}(k,k',E) = V^{js}_{ll'}(k,k') + \sum_{l''=|j-s|}^{j+s} \int_0^\infty \frac{dk'' V^{js}_{ll''}(k,k'') t^{js}_{l''l'}(k'',k',E)}{E - \frac{(k'')^2}{2\mu} + i0}. \quad (7)$$

Apart from the total angular momentum and spin, the parity is also conserved for the NN potential. Thus, Eq. (7) is either a set of two coupled integral equations for the spin-triplet case $s = 1$ (for $l,l' = |j-1|, j+1$) or an uncoupled equation for the spin-singlet ($s = 0$) and the spin-triplet ($s = 1$) channels with $l = j$.

To find the single- and coupled-channel t matrices, we introduce at first a partition of the continuum for the free Hamiltonian $\hat{h}_0$ onto nonoverlapping energy intervals (bins) $\{\mathfrak{D}_i \equiv [\mathcal{E}_{i-1},\mathcal{E}_i]\}_{i=1}^N$ (or the corresponding momentum bins $[k_{i-1},k_i]$)[1] and then construct the stationary wave-packet (WP) basis functions $|x^l_i;\alpha\rangle$ as integrals of free plane waves $|k\rangle$ over these bins with inclusion of the necessary spin-angular parts $|\alpha\rangle \equiv |l,s:j\rangle$ [8]:

$$\left|x^l_i,\alpha\right\rangle = \frac{1}{\sqrt{d_i}} \int_{k_{i-1}}^{k_i} dk |k,\alpha\rangle, \quad d_i = k_i - k_{i-1}. \quad (8)$$

It is easy to show that the WP states (8) form an orthonormal basis:

$$\left\langle x^l_i,\alpha \middle| x^{l'}_{i'},\alpha' \right\rangle = \delta_{ii'}\delta_{\alpha\alpha'}. \quad (9)$$

In such a basis, a simple finite-dimensional representation for the free resolvent $\hat{g}_0(E)$ takes the form [8]:

$$\hat{g}_0(E) \approx \sum_\alpha \sum_{i=1}^N \left|x^l_i,\alpha\right\rangle g_i(E) \left\langle x^l_i,\alpha\right|, \quad (10)$$

where the complex functions $g_i(E)$ can be found from the formula (A5) of the Appendix and depend on the discretization parameters $\mathcal{E}_i$ and total energy E only[2] [8]. By using the representation (10), it is easy to reduce the integral Eq. (7) to the matrix one (see also Ref. [16], where a similar approach was used in nuclear matter calculations).

Projecting out Eq. (7) onto the WP basis, one gets the matrix equation for the coupled-channel t matrix (and the corresponding equations for uncoupled cases):

$$t^{js}_{il,i'l'}(E) = V^{js}_{il,i'l'} + \sum_{l''=|j-s|}^{j+s} \sum_{i''} V^{js}_{il,i''l''} g_{i''}(E) t^{js}_{i''l'',i'l'}(E), \quad (11)$$

where $V^{js}_{il,i'l'} \equiv \langle x^l_i,\alpha|\hat{V}|x^{l'}_{i'},\alpha'\rangle$ and $t^{js}_{il,i'l'}(E) \equiv \langle x^l_i,\alpha|\hat{t}(E)|x^{l'}_{i'},\alpha'\rangle$ are matrix elements of the interaction and transition operator, respectively.

The off-shell t matrix can be found from the solution of the matrix Eq. (11):

$$t^{js}_{ll'}(k,k';E) \approx \frac{t^{js}_{il,i'l'}(E)}{\sqrt{D_i D_{i'}}}, \quad \begin{matrix} k \in \mathfrak{D}_i, \\ k' \in \mathfrak{D}_{i'}, \end{matrix} \quad (12)$$

where $D_i = \mathcal{E}_i - \mathcal{E}_{i-1}$ are widths of the corresponding energy intervals.

The respective S matrix is derived from the diagonal element of the WP t matrix:

$$S^{js}_{ll'}(E) \approx \delta_{ll'} - 2\pi i \frac{t^{js}_{il,il'}(E)}{D_i}, \quad E \in \mathfrak{D}_i. \quad (13)$$

However, such a procedure requires a separate matrix inversion at every energy E considered. So, if one needs to evaluate the coupled-channel t matrix at many energies (e.g., for any Faddeev or Faddeev-Yakubovsky calculation), the above direct way turns out somewhat time-consuming. This problem is also important in case of nuclear matter calculations where one has to calculate the reaction matrix for various center-of-mass momenta and also to carry out the numerous iterations to reach the self-consistency.

Thus, below we will show how to evaluate the off-shell t matrix without solving the scattering equations for each energy by using the Hamiltonian matrix diagonalization in an appropriate model space.

C. The resolvent of the total Hamiltonian

For fixed values of j and s, the total Hamiltonian can be written as a coupled-channel operator:

$$\hat{h}^{js}_{ll'} = \hat{h}^{js}_{0l}\delta_{ll'} + \hat{V}^{js}_{ll'}, \quad (14)$$

with a dimension d equal to 1 or 2 for uncoupled and coupled cases correspondingly.

The general idea of the wave-packet approach to find the total resolvent of some Hamiltonian $\hat{h}$ is a discretization of its continuum similarly to the free Hamiltonian case and a construction of *the scattering wave packets* by Eq. (A1) from the exact scattering wave functions. In this new WP representation, the resolvent of the Hamiltonian $\hat{h}$ has a diagonal

[1] We denote energy and momentum intervals with the same notation $\mathfrak{D}_i$.

[2] Although these explicit relations for $g_i(E)$ contain logarithmic singularities at the endpoints of the energy intervals, this finite-dimensional representation for the free resolvent allows one to reproduce a correct analytical structure of the initial operator. In particular, it has a proper discontinuity across the real positive energy semiaxis. With some additional averaging procedure [8], the representation (10) is valid at any energy E.

form with known eigenvalues (see Ref. [8] and the Appendix to the present paper). At the next step, the scattering WPs are approximated by pseudostates of the total Hamiltonian found in a free WP basis. Thus, by using the same free WP basis and employing the total Hamiltonian matrix diagonalization procedure, one can find finite-dimensional approximations both for the free and total Hamiltonian resolvents $\hat{g}_0$ and $\hat{g}$, respectively.

Being fully straightforward for a single-channel total Hamiltonian, this diagonalization approach requires some special consideration in a coupled-channel case because the continuous spectra of the free and total Hamiltonians are degenerated. So one has two different scattering wave functions at each energy E corresponding to different initial states. The ordinary pseudostate technique does not allow one to distinguish these different channel states. However, we have shown previously that special eigenchannel representation formalism can be employed here [8].

Indeed, one can introduce two different types of scattering states for the Hamiltonian (14) at given energy E: the scattering states $|\psi^l(E)\rangle$ (which include also spin-angular parts) corresponding to the incoming waves with a definite orbital momentum l and the scattering states $|\psi^\varkappa(E)\rangle$ defined in the so-called eigenchannel representation (ER) (which corresponds to a diagonal form of the total S matrix [14,17]), where $\varkappa$ is an eigenchannel index. For example, in case of the coupled-channel triplet NN interaction, the scattering states $|\psi^\varkappa(E)\rangle$ are linear combinations of the states $|\psi^l(E)\rangle$, e.g., eigenchannel states for the coupled channels ${}^3S_1$-${}^3D_1$, ${}^3P_2$-${}^3F_2$, etc.[3]

Further, by making use of the above eigenchannel representation in a coupled-channel case, one gets the following spectral expansion for the resolvent of the total Hamiltonian $\hat{g}(E)$:

$$\hat{g}^{js}(E) = \frac{|z_b\rangle\langle z_b|}{E-\epsilon_b} + \sum_{\varkappa=1}^{d}\int_0^\infty \frac{|\psi^\varkappa(E)\rangle\langle\psi^\varkappa(E)|}{E+i0-E'}dE', \quad (15)$$

which is *diagonal* with respect to the eigenchannel index $\varkappa$. In Eq. (15), ϵ_b is an energy of the bound state $|z_b\rangle$ (the deuteron). In the NN system, the bound-state term takes place for the triplet with $j=1$ channel, only.

To use further the WP technique with the pseudostate approximation, one has to prepare the discretization partitions of spectra in different coupled spin-angular channels in such a way that a coupled-channel free Hamiltonian matrix would have *a degenerate discrete spectrum* [8,14]. After switching on the interaction, these multiple discrete energy levels are split and form a set of paired levels (for two coupled channels [14]). So one can group the resulted coupled-channel pseudostates into two branches in the eigenchannel representation. We have shown [14] that such pseudostates obtained in the free WP basis can easily be related to scattering wave functions $|\psi^\varkappa(E)\rangle$. More definitely, these pseudostates can be considered as approximations for the *multichannel* scattering wave packets constructed from exact scattering wave functions (defined in the ER) of the coupled-channel total Hamiltonian $\hat{h}_{ll'}$ [see Eq. (A8) in the Appendix].

Thus, the diagonalization of the total Hamiltonian (14) matrix in the two-channel free WP basis $\{|x_i^l;l,s:j\rangle\}_{l=|j-s|}^{j+s}$ results in a set of pseudostates $|z_k^\varkappa,\tilde{\alpha}\rangle$ with eigenenergies $E_k^\varkappa$, which are expanded in free WP states:

$$|z_k^\varkappa,\tilde{\alpha}\rangle = \sum_{i,l} C_{ki}^{\varkappa l}|x_i^l,\alpha\rangle. \quad (16)$$

Here $\varkappa$ is an eigenchannel index and the total spin-angular part has the form $\tilde{\alpha}=\{\varkappa,s,j\}$.

With such a treatment of the multichannel pseudostates, a finite-dimensional representation for the total resolvent takes a diagonal form [8] both for single- and a coupled-channel cases:

$$g^{js}(E) \approx \frac{|z_b\rangle\langle z_b|}{E-\epsilon_b} + \sum_{\varkappa=1}^{d}\sum_{k=1}^{N_\varkappa}|z_k^\varkappa\rangle g_k^\varkappa(E)\langle z_k^\varkappa|, \quad (17)$$

where functions $g_k^\varkappa(E)$ are defined by Eq. (A10). It should be emphasized that the expansion (17) is not a polelike pseudostate approximation for the total resolvent but it corresponds to a disicretization of the coupled-channel continuous spectrum of the total Hamiltonian within the scattering wave-packet formalism (see the details in the Appendix). The latter formalism is similar to the above free WP approach for the free Hamiltonian spectrum discretization which results in the finite-dimensional representation (10) for the free resolvent. Moreover, the explicit formulas (A5) and (A10) for functions $g_k^\varkappa(E)$ are the same for cases of single- and coupled-channel scattering [8].

Finally, the representation of the total resolvent as a finite spectral sum, as in Eq. (17), allows a direct evaluation of the multienergy off-shell t matrix.

After carrying out the diagonalization procedure for the total Hamiltonian matrix at a fixed coupled-channel partial wave (j,s), the off-shell t matrix is found from the explicit relation [instead of solving Eq. (11)]:

$$t_{il,i'l'}^{js}(E) \approx V_{il,i'l'}^{js} + \frac{V_{il,\mathrm{b}}^{11}V_{i'l',\mathrm{b}}^{11}}{E-\epsilon_\mathrm{b}}\delta_{j1}\delta_{s1} + \sum_{\varkappa=1}^{d}\sum_{k=1}^{N_\varkappa}V_{il,k\varkappa}^{js}g_k^\varkappa(E)V_{i'l',k\varkappa}^{js}, \quad (18)$$

where $d=2$ or 1 for coupled or uncoupled channel, respectively. Here specific matrix elements of the interaction operator have been introduced: $V_{il,\mathrm{b}}^{js} \equiv \langle x_i^l,\alpha|\hat{V}|z_\mathrm{b}\rangle$ and $V_{il,k\varkappa}^{js} \equiv \langle x_i^l,\alpha|\hat{V}|z_k^\varkappa,\tilde{\alpha}\rangle$. They are calculated from the matrix elements of the interaction in the initial free WP basis by using Eq. (16), e.g.,

$$V_{il,k\varkappa}^{js} = \sum_{l',i'} C_{ki'}^{\varkappa l'}V_{il,i'l'}^{js}. \quad (19)$$

As an example for the application of the diagonalization procedure to find the NN scattering amplitudes we present in

[3]In nuclear physics, a conventional notation for these pair eigenstates is adopted as the so-called α state and β state. Here we use the general index $\varkappa$.

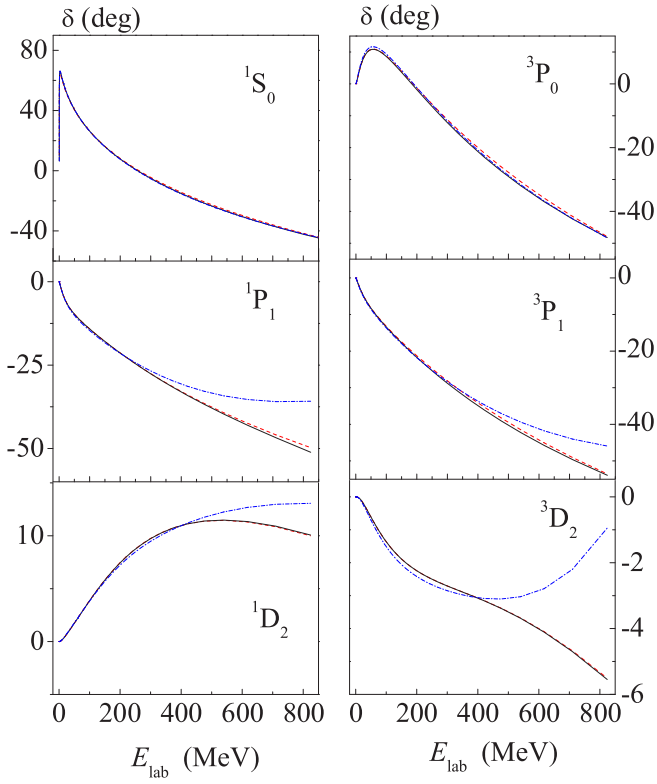

FIG. 1. The partial phase shift δ for uncoupled spin-singlet (left panel) and spin-triplet (right panel) channels derived from a total Hamiltonian diagonalization in the WP basis (solid curves) and from the direct numerical solution of the one-channel Lippmann-Schwinger equation (dashed curves) for the CD Bonn *NN* potential. The dash-dotted curves correspond to partial phase shifts evaluated for the Nijmegen *NN* potential.

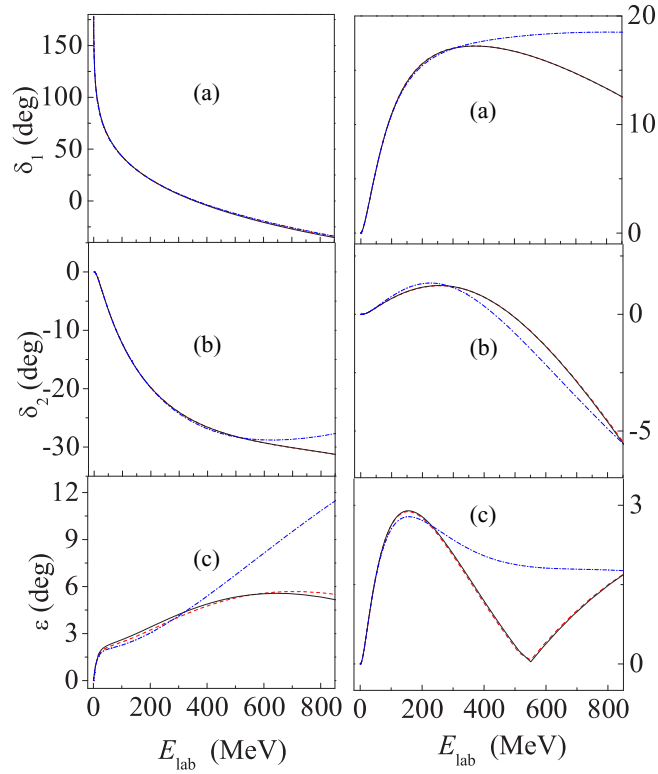

FIG. 2. The partial phase shifts δ_1 (a), δ_2 (b), and the mixing parameter ε (c) for the coupled spin-triplet channels $^3S_1$-$^3D_1$ (left panel) and $^3F_2$-$^3P_2$ (right panel) of the *NN* scattering found for the CD-Bonn and Nijmegen *NN* potentials. The notations of curves are the same as in Fig. 1.

Fig. 1 the partial phase shifts for the uncoupled spin-singlet and spin-triplet channels using the *NN* CD-Bonn potential [18]. To check the accuracy of the approach, we compare in this figure the results of the direct solution for the integral Lippmann-Schwinger equation in a matrix form (11) (which has to be solved at the various energies independently) with results of a single diagonalization for the respective *NN* coupled-channel Hamiltonian in the very broad energy interval of laboratory energy $E_{\rm lab}$ from zero up to 800 MeV. In these calculations, the free WP bases of the dimension $N = 100$ in every partial wave have been used. As the discretization mesh, we employed here the Tchebyshev grid (see for the details Ref. [8]).

It can be seen that the results for the direct and diagonalization solutions are almost indistinguishable from each other in the whole energy region studied. We have also added to Fig. 1 the partial phase shifts evaluated for the Nijmegen II *NN* potential [19]. The phase shifts derived from the different potentials agree mainly in the energy region, in which they both were fitted to the experimental data. The different behavior of the phase shifts for energies above 350 MeV is well known.

In Fig. 2 the coupled-channel phase shifts and mixing angle ε (in the Stapp parametrization) for the spin triplet channels of *NN* scattering with CD-Bonn potential are displayed and compared to solutions of the Lippmann-Schwinger equation in a matrix form Eq. (11). The very good accuracy which the diagonalization technique can reach in scattering calculations is obvious also for the coupled-channel cases.

The clear advantage of the diagonalization technique as compared to the conventional solution of the LSE equation is evident, in particular, if one has to solve the LSE at many energies as it is in the case, e.g., for the calculation of integral kernels of Faddeev-Yakubovsky three- and many-body integral equations. As an example we refer to the three-body discrete Faddeev calculations [8], where we have used the finite-dimensional approximation for the total resolvent (17) derived from the Hamiltonian diagonalization procedure.

III. SOLVING THE BETHE-GOLDSTONE EQUATION BY A MATRIX DIAGONALIZATION

Let us consider a case of infinite symmetrical nuclear matter at zero temperature, where we study the respective Bethe-Goldstone integral equation for the Brueckner reaction matrix [2,3]:

$$T(\mathbf{k},\mathbf{k}';K,W_0) = V(\mathbf{k},\mathbf{k}') + \int d^3k'' V(\mathbf{k},\mathbf{k}'') \times \frac{Q(\mathbf{k}'',K)T(\mathbf{k}'',\mathbf{k}';K,W'')}{W_0 + i0 - H_0(\mathbf{k}'',\mathbf{K})}, \quad (20)$$

where $\mathbf{K} = \frac{1}{2}(\mathbf{k}_1 + \mathbf{k}_2)$ and $\mathbf{k} = \frac{1}{2}(\mathbf{k}_2 - \mathbf{k}_1)$ are the center-of-mass (c.m.) and relative momenta, respectively, W_0 is the starting energy, $H_0(\mathbf{k}'', K)$ defines the energy of the intermediate state with relative momentum $\mathbf{k}''$, and $Q(\mathbf{k}'', K)$ corresponds to the Pauli-projection operator:

$$Q(\mathbf{k}, K) = \theta(|\mathbf{k} + \mathbf{K}| - k_F)\theta(|\mathbf{k} - \mathbf{K}| - k_F), \tag{21}$$

which excludes particle states forbidden by the Pauli principle, so that k_F is the Fermi momentum. Because of the appearance of the Pauli projection operator in the kernel of Eq. (20), the c.m. momentum $\mathbf{K}$ is not separated out here (as it was for the LSE) but it is still conserved. Equation (20) is traditionally solved in the momentum space formed by the relative momentum $\mathbf{k}$ while the absolute value of the c.m. momentum K in Eq. (20) plays the role of an external parameter, in addition to the starting energy W_0.

In most of the calculations, the so-called angle-average approximation for the Pauli operator Q is assumed [2]:

$$Q(k, K) = \begin{cases} 0, & k \leqslant k_0, \\ \min\left\{1, \frac{k^2 + K^2 - k_F^2}{2kK}\right\}, & k > k_0, \end{cases} \tag{22}$$

where $k_0 = \sqrt{k_F^2 - K^2}$. If furthermore one considers a spectrum of particle states defined by $H_0(\mathbf{k}, K)$, which is also independent on the angle between the corresponding relative $\mathbf{k}$ and c.m. momentum $\mathbf{K}$ the Bethe-Goldstone equation is symmetric under rotation and can easily be solved in a partial wave expansion (see below) with matrix elements of the resulting reaction matrix diagonal in this partial wave basis with respect to j and s. In the present study, we will also take advantage of this angle-average approximation. Note, however, that an extension of the formalism to an exact treatment of Q and an angle-dependent energy term H_0 is straightforward.

It should be stressed that the operator $\hat{Q}$ in this angle-average approximation is not a projection operator because it does not satisfy the relation $\hat{Q}^2 = \hat{Q}$, but it can be considered in the relative momentum space as an operator $\hat{Q}(K)$ depending on the c.m. momentum value.

The energies in the denominator of Eq. (20) W_0 and $H_0(k, K)$ are usually defined through the Brueckner-Hartree-Fock (BHF) single-particle (sp) energy,

$$\varepsilon(k_1) = \frac{k_1^2}{2m} + \mathrm{Re}(U(k_1, \omega = \varepsilon(k_1))), \tag{23}$$

where the self-energy U is defined in terms of the reaction matrix itself:

$$U(k_1, \omega) = \int_{k_2 \leqslant k_F} d^3k_2 T(\mathbf{k}, \mathbf{k}; K, W_0 = \omega + \varepsilon(k_2)). \tag{24}$$

In the last equation, the integral over $\mathbf{k}_2$ should be restricted to the hole states, i.e., single-particle states inside the Fermi sphere [3].

While the on-shell definition of the energy variable ω in Eq. (23) is well established for the single-particle energies of the hole states by the Bethe-Brandow-Petschek theorem [20], the corresponding choice for the spectrum of the particle states with momenta larger than k_F, which are needed to define H_0, was a matter of lengthy discussion in the literature. Two different choices have been discussed:

(i) The conventional choice representing the single-particle energies for the particle states by the kinetic energy only,

$$\varepsilon(k_1) = \frac{k_1^2}{2m}.$$

With this choice one obtains a gap at $k_1 = k_F$ as the attractive single-particle potential $U(k_1)$ defined in Eq. (24) is taken into account for the hole states ($k_1 < k_F$) but is ignored for the particle states. Therefore this choice was also denoted as the "gap" spectrum.

(ii) The "continuous" or gapless choice, in which the definition of the single-particle energy according to Eq. (24) is also applied to the particle states with $k_1 > k_F$.

The discussion of the optimal choice for the single-particle potential was essentially settled with the observation of Baldo *et al.* [21] demonstrating that the effect of three-nucleon correlations is reduced considering the continuous choice. Therefore this continuous choice has become the standard choice in BHF calculations.

In any case one obtains a monotonic rise of the single-particle energy $\varepsilon(k_1)$ as a function of the momentum k_1 and the matrix elements of T are complex only for energies ω and corresponding starting energies W_0, which are needed for the evaluation of the particle states. This implies that the BHF single-particle potential (24) is real for the hole states with momenta $k_1 < k_F$. For energies ω larger than the Fermi energy $\varepsilon_F = \varepsilon(k_F)$ the single-particle potential $U(k_1)$ yields an imaginary component and this complex self-energy $U(k_1, \omega)$ was used to evaluate the optical model potential for nucleon-nucleus scattering [22].

Note that the solution of the Bethe-Goldstone Eq. (20) and the evaluation of the single-particle potential Eq. (24) must be done in a self-consistent way because the BGE requires the knowledge of the single-particle spectrum and the evaluation of the single-particle energies requires the knowledge of the reaction matrix T, that is the solution of the Bethe-Goldstone equation. The self-consistent solution can be obtained in an iterative way recalculating in each iteration step the single-particle spectrum until the resulting spectrum will agree with the spectrum which is used in the Bethe-Goldstone equation.

In this iteration procedure the single-particle spectrum to be used in Eq. (20) was often parametrized in terms of an effective mass m^*:

$$\varepsilon_{app}(k_1) = \frac{k_1^2}{2m^*} + U_0. \tag{25}$$

This parametrization simplifies the iteration procedure and ensures that the energy denominators used in the Bethe-Goldstone Eq. (20) do not depend on the angle between relative and c.m. momentum of the interacting pair of nucleons. This is a very useful feature together with the angle-average definition of the Pauli operator (22). It was observed [3], however, that effective-mass parametrization is not very accurate (see also discussion below).

When the iteration scheme discussed above is converged, the binding energy per nucleon (the equation of state) can be found with the resulting sp spectrum using the relation:

$$\frac{E}{A} = \frac{3}{k_F^3}\int_0^{k_F} k^2\, dk\, \frac{1}{2}\left[\frac{k^2}{2m} + \varepsilon(k)\right]. \tag{26}$$

A. The resolvent operator

For a standard BHF calculation, it is sufficient to solve the BGE by means of standard techniques for solving integral equations as, e.g., it was introduced by Haftel and Tabakin [2]. Calculations beyond the standard BHF calculations, like the evaluation of the self-energy beyond lowest order hole-line expansion, or the solution of the three-body Bethe-Faddeev equation or the evaluation of the fully off-shell behavior of the self-energy, all require the determination of the reaction matrix at various starting energies. Thus, the discrete wave-packet representation should be useful for such multifold calculations; also it allows one to obtain a different view on the solution of the Bethe-Goldstone equation. For this aim, we will take a brief look at the propagator for the Bethe-Goldstone equation or the resolvent operator for the corresponding total Hamiltonian.

Let us introduce the free Hamiltonian for two noninteracting nucleons in nuclear matter for a fixed value of the c.m. momentum K:

$$\hat{H}_0(K) = \int d^3k |\mathbf{k}\rangle H_0(\mathbf{k},K)\langle\mathbf{k}|, \tag{27}$$

where $|\mathbf{k}\rangle$ are plane wave state for the relative momentum $\mathbf{k}$ and energy terms $H_0(\mathbf{k},K) = \varepsilon(|\mathbf{k}-\mathbf{K}|) + \varepsilon(|\mathbf{k}+\mathbf{K}|)$ are defined by means of a given sp potential.

Then, Eq. (20) can be rewritten in the operator form,

$$\hat{T}(K,W) = \hat{V} + \hat{V}\,\hat{Q}(K)\hat{G}_0(K,W)\hat{T}(K,W), \tag{28}$$

where the free resolvent $\hat{G}_0(K,W)$ is defined as usually as $\hat{G}_0(K,W) = [W + \mathrm{i}0 - \hat{H}_0(K)]^{-1}$ for the free Hamiltonian (27). Below we will omit the explicit dependence of operators on K where is possible to simplify notations.

It can easily be proven that if one introduces some operator $\hat{G}(W)$ which satisfies the operator equation:

$$\hat{G}(W) = \hat{Q}\hat{G}_0(W) + \hat{Q}\hat{G}_0(W)\hat{V}\hat{G}(W), \tag{29}$$

then the solution of Eq. (28) (the reaction matrix) can be found from the formal relation,

$$\hat{T}(W) = \hat{V} + \hat{V}\hat{G}(W)\hat{V}, \tag{30}$$

similarly to the ordinary t-matrix case.

Thus, if one would find some convenient way for the evaluation of the operator $\hat{G}(W)$ then the reaction matrix could be calculated straightforwardly from Eq. (30).

For this purpose, let us introduce two orthogonal subspaces $\mathcal{H}_\Gamma$ and $\mathcal{H}_Q$ of the total momentum space $\mathcal{H}$ with respect to an action of the operator $\hat{Q}(K)$. Here $\mathcal{H}_\Gamma$ is the null space of $\hat{Q}(K)$ (it includes the states $|\mathbf{k}\rangle$ for which $\hat{Q}(K)|\mathbf{k}\rangle = 0$), while $\mathcal{H}_Q$ is its orthogonal complement (i.e., it includes the Pauli-allowed states). Below we will denote projections of the operators onto these subspaces with additional subindex Γ or Q, respectively.

Because $\hat{Q}$ commutes with $\hat{G}_0(W)$, it becomes clear from Eq. (29) that $\hat{G}(W)$ commutes with $\hat{Q}$ too. Thus, Eq. (29) should be considered in the subspace $\mathcal{H}_Q$ only. Because of the definition, the inverse operator $\hat{Q}^{-1}$ and also the operators $\hat{Q}^{\frac{1}{2}}$ and $\hat{Q}^{-\frac{1}{2}}$ exist in this subspace.

Then Eq. (29) can be rewritten in a symmetric form:

$$\hat{Q}^{-\frac{1}{2}}\hat{G}\hat{Q}^{-\frac{1}{2}} = \hat{G}_{0Q} + \hat{G}_{0Q}\;\hat{Q}^{\frac{1}{2}}\hat{V}\hat{Q}^{\frac{1}{2}}\;\hat{Q}^{-\frac{1}{2}}\hat{G}\hat{Q}^{-\frac{1}{2}},$$

which is similar to the resolvent identity (3). So it is straightforward to derive the following explicit form for the $\hat{G}(K,W)$ operator:

$$\hat{G}(K,W) = \hat{Q}^{\frac{1}{2}}[W + \mathrm{i}0 - \hat{H}_{0Q}(K) - \hat{Q}^{\frac{1}{2}}\hat{V}\hat{Q}^{\frac{1}{2}}]_Q^{-1}\hat{Q}^{\frac{1}{2}}, \tag{31}$$

where the inverse operator is defined in $\mathcal{H}_Q$. Further, one can introduce the spectral expansion for the operator $\hat{G}(K,W)$ in terms of eigenstates of the following effective Hamiltonian $H_Q(K)$:

$$\hat{H}_Q(K) = \hat{H}_{0Q}(K) + \hat{Q}^{\frac{1}{2}}(K)\hat{V}\,\hat{Q}^{\frac{1}{2}}(K), \tag{32}$$

which is defined in the $\mathcal{H}_Q$ [as well as $\hat{H}_{0Q}$ is a part of the free Hamiltonian (27) in $\mathcal{H}_Q$].

The operator (31) is nothing else as an analog of the total resolvent operator $g(E)$ used in an ordinary scattering problem. Finally, the reaction matrix can be found in this formalism using the explicit formula:

$$\hat{T}(K,W) = \hat{V} + \hat{V}\,\hat{Q}^{\frac{1}{2}}[W + \mathrm{i}0 - \hat{H}_Q(K)]_Q^{-1}\hat{Q}^{\frac{1}{2}}\hat{V}, \tag{33}$$

which is very convenient because the energy and K dependencies are separated in it.

Thus, one can recognize in the final Eq. (33) an analog of Eq. (4) for the transition operator in free space which relates the t matrix and the total resolvent $\hat{g}$. So, in quite a similar manner, one can replace the multiple solutions of the BGE (20) at many values of relative momentum k with a single diagonalization of the Hamiltonian matrix $\hat{H}_Q(K)$ in $\mathcal{H}_Q$ subspace, no matter which particular form of the Pauli-exclusion operator $\hat{Q}$ is used (i.e., the angle-averaged or the exact form).

B. Evaluation of the reaction matrix in the discrete WP representation

Here we apply the discrete formalism, developed in Sec. II, to derive the reaction matrix using a partial wave decomposition in Eq. (33). For our illustrative purpose, the angle averaged approximation for the $\hat{Q}(K)$ operator [2] is used. In that case, its momentum eigenvalues do not depend on spin-angular quantum numbers and have the form displayed in Eq. (22).

Thus, the $\mathcal{H}_Q$ subspace includes plane wave states with relative momentum $k > k_0$ [see Eq. (22)] and it is convenient to introduce the discretization bins in such a way that the momentum k_0 should coincide to the endpoint of some bin. Thus, we have $\{|x_i\rangle\}_{i=1}^{N_1}$ and $\{|x_i\rangle\}_{i=N_1+1}^{N}$ sets as the bases for subspaces $\mathcal{H}_\Gamma$ and $\mathcal{H}_Q$, respectively, and $k_{N_1} = \sqrt{k_F^2 - K^2}$.

In case of the angle-averaged projector, the matrix elements of the operator $\hat{Q}(K)$ can be found as follows:

$$\hat{Q}(K) = \sum_{\alpha} \sum_{i=N_1+1}^{N} |x_i,\alpha\rangle Q_i(K) \langle x_i,\alpha|,$$

$$Q_i = \frac{1}{d_i} \int_{k_{i-1}}^{k_i} dk\, Q(k,K), \quad d_i = k_i - k_{i-1}. \tag{34}$$

If furthermore we assume that also the eigenvalues of the free Hamiltonian $\hat{H}_0$ are independent of the angle between relative and c.m. momenta, the matrix elements of the effective Hamiltonian (32) take the form for a coupled-channel NN interaction:

$$[H]^{js}_{il,i'l'} = [H_0]_i \delta_{ii'} \delta_{ll'} + \sqrt{Q_i} V^{js}_{il,i'l'} \sqrt{Q_{i'}}, \tag{35}$$

where $i,i' = N_1+1,\ldots,N$, $l,l' = |j-s|, j+s$ (or $l = l' = j$ for uncoupled channels), and $[H_0]_i$ is the matrix element of the free Hamiltonian $\hat{H}_0$.

The continuous spectrum of the effective Hamiltonian (32) starts at the minimal value of $H_0(k,K)$ for the Pauli-allowed space. This threshold value is equal to $2\varepsilon_F$. The diagonalization of this Hamiltonian matrix in $\mathcal{H}_Q$ subspace results either in a set of one-channel pseudostates $|z^l_k\rangle$ with energies E^l_k or in a set of coupled-channel pseudostates $|z^\varkappa_k\rangle$ with eigenvalues $E^\varkappa_k$ both expanded over the free WP basis (similarly to the case of the ordinary NN scattering in a free space discussed in Sec. II). Also the effective Hamiltonian may have bound states, i.e., the states $|z^b_n\rangle$ with energies E_n which are located below the threshold (see below).

Thus, in the above discrete WP representation, the total resolvent $\hat{G}(K,W)$ from Eq. (31) can be approximated by the following superposition:

$$\hat{G}^{js}(K,W) \approx \sum_{n=1}^{N_b} \frac{|z^b_n\rangle\langle z^b_n|}{W - E_n} + \sum_{\varkappa=1}^{d} \sum_{k=1}^{N_{\rm eff}} |z^\varkappa_k\rangle g^\varkappa_k(W) \langle z^\varkappa_k|, \tag{36}$$

where the multiplicity of the continuum d is equal to 2 or 1. $N_{\rm eff}$ is a number of pseudostates of the effective Hamiltonian in each channel.

Finally, by using Eq. (33), one gets a simple relation for the Brueckner reaction matrix which is conveniently represented as sum of three terms,

$$\hat{T} = \hat{V} + \hat{T}^b + \hat{T}^c, \tag{37}$$

where $\hat{T}^b$ and $\hat{T}^c$ correspond to bound-state and continuum contributions, respectively. In the wave-packet partial wave representation they have the following forms:

$$T^{b,js}_{il,i'l'}(K,W) = \sum_{n=1}^{N_b} \frac{\tilde{V}^{js}_{il,n} \tilde{V}^{js}_{i'l',n}}{W - E_n}, \tag{37a}$$

$$T^{c,js}_{il,i'l'}(K,W) = \sum_{\varkappa,k} \tilde{V}^{js}_{il,k,\varkappa} g^\varkappa_k(W) \tilde{V}^{js}_{i'l',k\varkappa}, \tag{37b}$$

where the matrix elements of the interaction are calculated by using the following relations,

$$\tilde{V}^{js}_{il,k\varkappa} \equiv \langle x^l_i | \hat{V} \hat{Q}^{\frac{1}{2}} | z^\varkappa_k \rangle = \sum_{l',i} V^{js}_{il,i'l'} \sqrt{Q_{i'}} C^{l'\varkappa}_{i'k}, \tag{38}$$

and the similar formulas are for the bound-state part.

Let us mention that it is not necessary to employ the WP basis states in the $\mathcal{H}_\Gamma$ subspace. The reaction matrix is determined from Eq. (37) in the momentum representation in which the finite-dimensional approximation (36) via pseudostates for $\hat{G}(K,W)$ is employed.

As is noted above (in particular for the so-called continuous choice of the energy spectrum of particle and hole states) the spectrum of the effective Hamiltonian (35) may exhibit eigenvalues E_n, which are below the threshold of the continuum:

$$E_n - 2\varepsilon_F < 0. \tag{39}$$

Such bound states can lead to numerical instabilities in conventional methods for solving the BHF equations, while they just receive special attention in the calculational scheme presented here according to the $\hat{T}^b$ term. These bound states embedded in the medium of nuclear matter are also of interest from a physical point of view. They have been recently studied in the literature (see, e.g., [23]). For the calculational scheme presented here, these bound states are a kind of spin-off product and we will discuss them below.

IV. SOME ILLUSTRATIVE EXAMPLES FOR SYMMETRIC NUCLEAR MATTER

The examples which we are presenting in this section have been evaluated for isospin symmetric nuclear matter at various densities, which are described in terms of the corresponding Fermi momentum k_F. The angle-average Pauli operator (22) is employed and we consider for this explorative presentation of the method the NN propagators with simple averages of the corresponding two-nucleon energies, which are independent on the angle between relative and c.m. momenta, so that the solution of the Bethe-Goldstone equation can be done in the partial wave basis. All results have been obtained for the CD Bonn potential [18] considering just the proton-neutron interaction in all channels. In practical calculations, the free WP basis of the dimension $N = 100$ for the relative momentum variable k was used (for every partial wave) which occurred to be sufficient to reproduce accurately continuous energy dependencies as well as to approximate correctly the bound states.

A. Bound two-particle states

At first, we want to make a few remarks on the appearance of two-nucleon bound state configurations in the medium of nuclear matter. As already noted above these states emerge as a kind of byproduct in our calculations. From experiment one knows that in the vacuum there is only one bound state, the deuteron. It is of course a common feature of all realistic NN interactions that they reproduce this bound state at -2.224 MeV in the $^3S_1$-$^3D_1$ channel and do not generate bound states in any other partial wave.

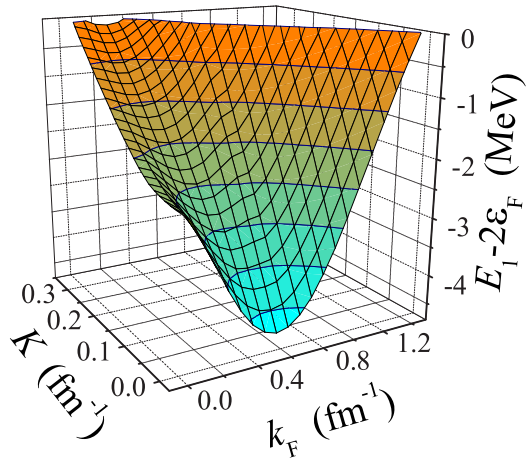

FIG. 3. The energy of the two-nucleon bound states in nuclear matter in the deuteron channel as a function of c.m. momentum K and Fermi momentum k_F.

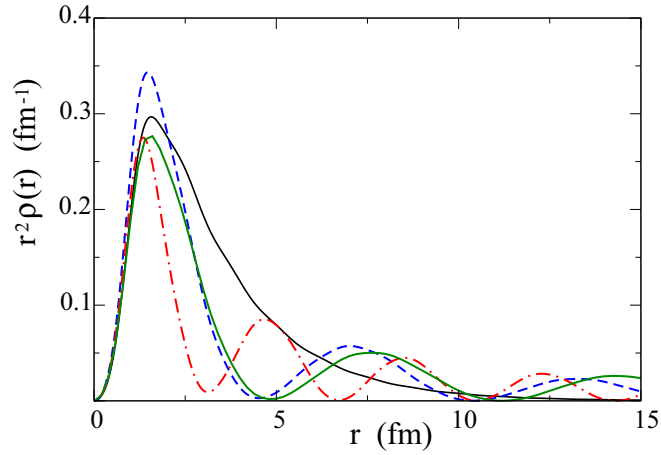

FIG. 4. The density of the quasideuteron as a function of relative distance r for various Fermi momenta k_F. The results for $k_F = 0.5$ fm^{-1} (blue dashed line) and 0.8 fm^{-1} (red dashed dotted line) have been determined for a c.m. momentum $K = 0$ and are compared to the corresponding density profile of the deuteron in free space (black solid line). For $k_F = 0.5$ fm^{-1}, a profile for c.m. momentum $K = 0.3$ fm^{-1} (green line) is presented also. Note that the density $\rho(r)$ is multiplied by r^2 to enhance the density at large r.

Naively, one may expect that the Pauli principle reduces the available phase space and therefore will make it more difficult to generate bound states. However, in addition to the *NN* interaction, a very important ingredient for the formation of bound states is the density of states close to the threshold. This density increases in nuclear matter with increasing Fermi momentum. Therefore the energy of the bound state, E_k^x-$2\varepsilon_F$ becomes more attractive at low densities and exhibits a minimum of around -4.5 MeV at $k_F = 0.6$ fm^{-1} as can be seen from the results displayed in Fig. 3. Because of the Pauli principle effect discussed above, the binding energy gets less attractive for larger values of k_F. The quasideuteron states, however, remain up to $k_F = 1.3$ fm^{-1}, which is just below the empirical value of the saturation density.

The binding energy of the quasideuterons in the medium is very sensitive to the c.m. momentum under consideration and decreases very rapidly with increasing c.m. momentum K.

Examples for the density profile for quasideuteron states are displayed in Fig. 4 as functions of the distance between the nucleons and compared to the corresponding density distribution for the "free" deuteron. The most pronounced difference between the density profiles for the deuteron and the bound-state structures in the nuclear medium are the ripples in the latter. The scale of these ripples is determined by the relative momenta slightly above the Fermi momentum, which dominates the momentum distribution in the wave functions of these states. The decrease of the density with increasing r, on the other hand, reflects the binding energy of the states and it is weaker for the states with the larger c.m. momentum.

All these bound-state structures in the medium discussed so far have been evaluated assuming a pure kinetic energy for the noninteracting nucleons also in the nuclear medium. Inclusion of the single-particle self-energy tends to reduce the binding energies of the bound-state structures, as the self-energy lowers the density of states around the Fermi energy. The momentum dependence of the self-energy is often expressed in terms of an effective mass m^* [see Eq. (25) and discussion below]. A detailed evaluation of the single-particle potential yields an enhancement of this effective mass close to the Fermi energy ($m^* \to m$), which originates mainly from the energy dependence of the self-energy (E mass) [6] (see also discussion below). Therefore the calculations ignoring the effects of the single-particle potential may be not too bad, because the effects of the single-particle potential drop out when they are in the difference $E_B = E_n - 2\varepsilon_F$. In fact, while the calculation of the quasideuteron in the nuclear medium at $k_F = 1.0$ fm^{-1} ($K = 0$) yields an energy of -2.9 MeV when calculated without self-energies included, the corresponding calculation considering the complete momentum and energy dependence of the self-energy yields -1.8 MeV.

While there is only one bound state in the vacuum, the deuteron, in the nuclear medium one may also obtain a bound state in other partial waves. In our calculations, we observe bound states also in the $^1S_0$ channel with isospin $\tau = 1$. From the results displayed in Fig. 5 one can see that the CD Bonn interaction yields bound-state configurations in this channel for Fermi momenta k_F up to 1 fm^{-1} with a maximal binding energy of 0.6 MeV, which is considerably weaker than in the case of the quasideuteron.

The occurrence of these quasibound states formed as a superposition of particle-particle states can be interpreted as an indicator for the onset of the superfluid phase and the formation of pairing correlations in the corresponding channels. It should be noted, however, that a consistent description of short-range and pairing correlations requires the extension of the normal single-particle Greens function, to include the anomalous part [5,24–26]. Such a description, taking into account the depletion of the Fermi sea from short-range and pairing correlations, can be achieved within a self-consistent evaluation of Greens function [27,28] and requires an extension of the Bethe-Goldstone equation to include particle-particle and hole-hole ladders. It is a challenge

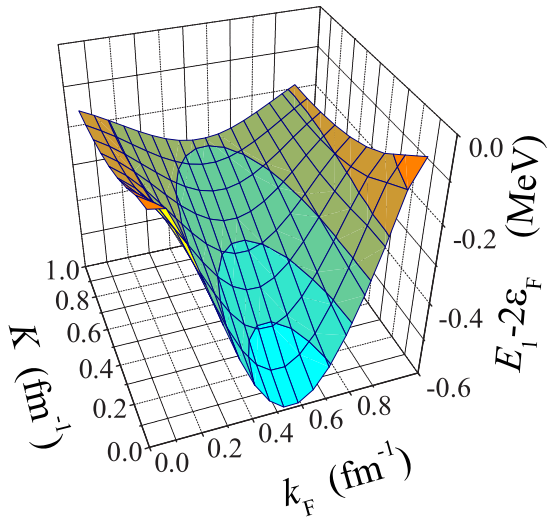

FIG. 5. The energy of the bound two-neutron states in the $^1S_0$ channel as a function of c.m. momentum and the Fermi momentum.

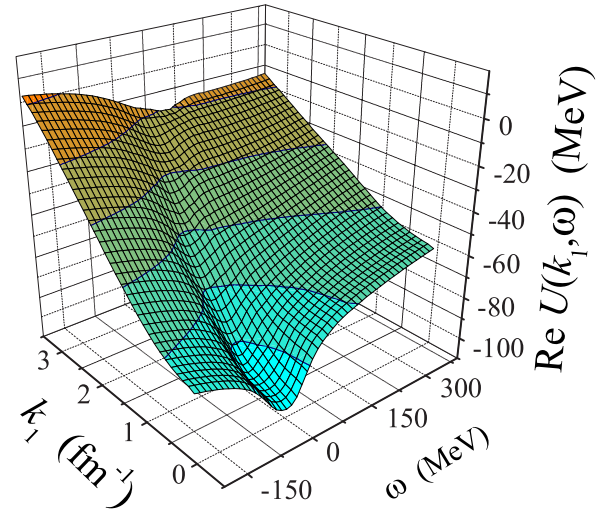

FIG. 6. Real part of nucleon self-energy as a function of momentum and energy, calculated for a Fermi momentum $k_F = 1.3$ fm^{-1}.

to extend the technique which was used in this work to include hole-hole ladders as well.

B. Discussion of the single-particle self-energy

One of the major advantages of the present scheme for solving the Bethe–Goldstone equation (20) is its efficiency whenever the reaction matrix is needed for various values of the energy parameter W. Therefore it is very easy with this approach to evaluate the whole energy and momentum dependence of the real and imaginary part of the single-particle potential or nucleon self-energy $U(k_1,\omega)$ as defined in (24).

The explicit formula for the self-energy (24) in the case of the angle-averaged Pauli projector can be rewritten in a form:

$$U(k_1,\omega) = \frac{2}{k_1}\sum_{jsl}(2j+1)(2\tau+1)\int_{\Omega(k_1)} dk dK k K, \times T_{ll}^{js}(k,k;K,W=[\omega+H_0(k,K)-e(k_1)]), \tag{40}$$

where the integration domain $\Omega(k_1)$ over k and K depends on the sp momentum k_1 value [2]. By using a discrete wave-packet representation for the reaction matrix and also some integration mesh $\{K_n\}$ with weights $\{\Delta K_n\}$ for the c.m. momentum, the explicit relation takes the form of a discrete sum:

$$U(k_1,\tilde{\omega}+e(k_1)) = \frac{2}{k_1}\sum_{jsl}(2j+1)(2\tau+1), \times \sum_{i,n} T_{il,il}^{js}(K_n,\tilde{\omega}+H_0(k_i,K_n))\Delta K_n. \tag{41}$$

Here matrix elements $T_{il,il}^{js}$ are defined by Eq. (37). It is straightforward to extract explicitly the Hartree–Fock part (caused by the bare interaction $\hat{V}$ only) and the bound-state part from the self-energy by using this explicit formula. We note also that the diagonalization procedure should be done for every value of K_n and the matrix elements for different k_i and $\tilde{\omega}$ are calculated by using just the same system of pseudostates of the effective Hamiltonain.

As an example we show in Figs. 6 and 7 the real and the imaginary parts of the self-energy U calculated at $k_F = 1.3$ fm^{-1} for various sp momenta k_1 and energies ω. The pole structure in the Bethe-Goldstone equation leads to an imaginary part only at energies ω above the Fermi energy ε_F, which is around -37 MeV in our example. This pole structure is also important for the energy dependence of the real part of U. It is seen that Re $U(k_1,\omega)$ is decreasing when the energy ω is rising being negative, has a minimum around $\omega = 0$, and then rises at positive values of ω.

As a consequence, the momentum dependence of the single-particle potential $U(k_1,\omega)$ at a fixed value of ω is much stronger than that for the self-consistent definition of the energy variable

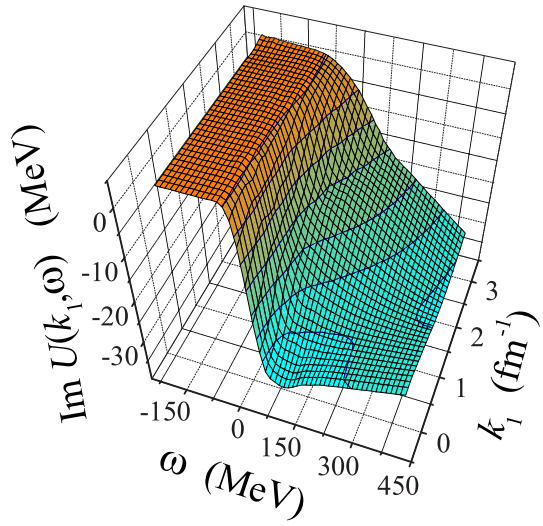

FIG. 7. Imaginary part of nucleon self-energy as a function of momentum and energy, calculated for a Fermi momentum $k_F = 1.3$ fm^{-1}.

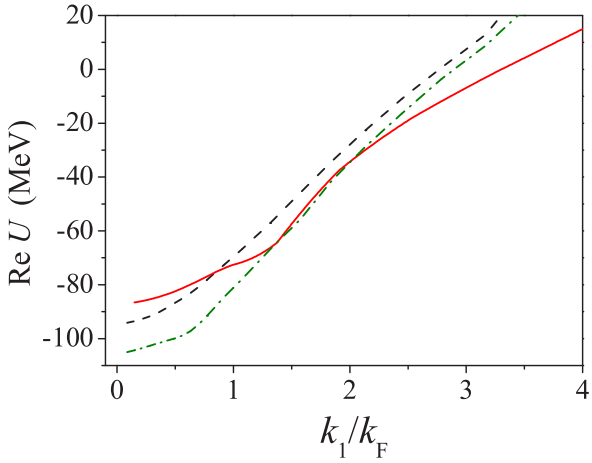

FIG. 8. Real part of the self-energy, calculated at fixed energies $\omega = -50$ MeV (dashed curve) and $\omega = 0$ MeV (dash-dotted curve) and found self-consistently following Eq. (24) (solid curve). Example for a Fermi momentum k_F =1.3 fm^{-1}.

according to Eq. (24) if we consider momenta below or slightly above the Fermi momentum. This is visualized in Fig. 8, in which we compare results for Re $U(k_1,\omega)$ for different energies ω with a single-particle potential found self-consistently.

This feature is well known and was discussed in the literature as an enhancement of the effective mass at the Fermi energy from the energy dependence of the self-energy or the so-called E-mass effect [6,29].

C. Calculation of the sp potential and the equation of state

As another example, we calculate the self-consistent sp potential and the equation of state by using the simple effective mass approximation for the sp energy at each iteration step. However, to check the reliability of this technique, two types of such an approximation have been employed, which differ by the maximal single-particle momentum value $k_1^{\max}$ used in the fitting of the effective mass parameters: $k_1^{\max} = 1.5k_F$ (the calculation 1) and $k_1^{\max} = 4k_F$ (the calculation 2).

It turns out that case 1 in which one makes use of the smaller fitting interval leads to a slightly smaller effective mass ($m^*/m = 0.694$ at $k_F = 1.3$ fm^{-1}) than in case 2 where one gets $m^*/m = 0.746$ (here m is the nucleon mass). In Figs. 9(a) and 9(b) the real and imaginary parts of the sp potentials calculated from self-consistent iterations by using these two approximations in energy terms H_0 are represented. One observes clearly that the shape in these figures is somewhat similar. The calculation 2, however, yields slightly larger absolute values for the real and imaginary parts. The differences seem to be small in this figure. Note, however, that the real part of the self-energy in calculation 2 is up to 2 MeV more attractive than the corresponding values for calculation 1.

These differences become even more visible in the binding energy dependence of the Fermi momentum k_F obtained from the corresponding sp potentials by using the formula (26). In Fig. 10, we compare the results of our discrete

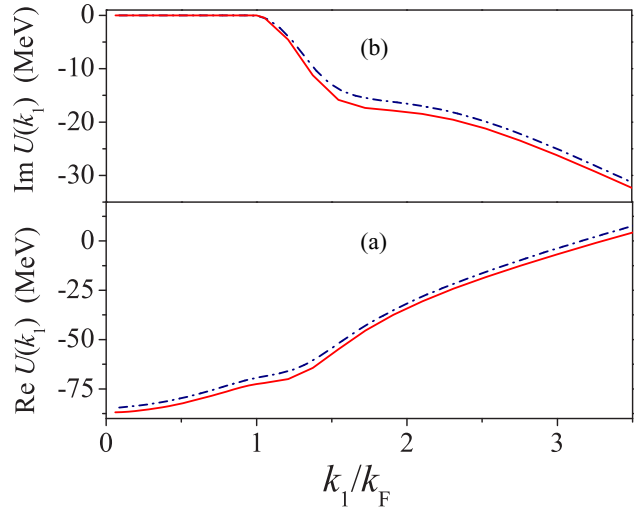

FIG. 9. Real (a) and imaginary (b) parts of the sp potential calculated self-consistently by using the effective mass approximations according to calculations 1 (dash-dotted curve) and 2 (solid curve).

wave-packet technique using the above two approximations 1 and 2 with the results of the fully self-consistent approach from Refs. [6,30], where angle-independent energy terms in the BGE with the exact nonaveraged Pauli projector have been used. The agreement of the latter results with the EOS found in the WP approach for calculation 2 is somewhat good, while calculation 1 with a shorter fitting interval for the effective mass approximation results in a smaller binding energy. This reflects a real problem with the effective mass approximation.

Thus, we have demonstrated clearly that the diagonalization technique developed here is very useful for evaluation of the

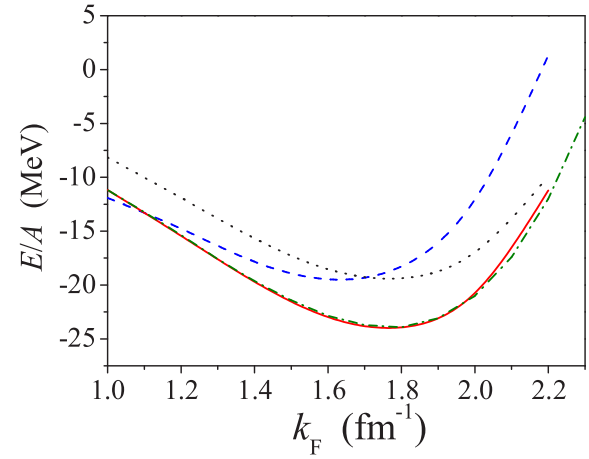

FIG. 10. Binding energy per nucleon calculated via the wave-packet diagonalization technique for the effective mass approximations in calculations 1 (dashed curve) and 2 (solid curve) in comparison with the results for the conventional sp spectrum choice (dotted curve). The dash-dotted curve corresponds to the results of the fully self-consistent calculations for the continuous choice from Refs. [6,30].

Brueckner reaction matrix and the single-particle spectrum in nuclear matter at various densities. However, the accurate treatment of the nuclear matter EOS still requires also calculation of three- and few-body correlation contributions for the binding energy in nuclear matter. This leads to solving complicated three-body equations for the reaction matrix such as the Bethe-Faddeev ones. A direct solution of the latter equations for realistic NN and $3N$ interactions in fully self-consistent scheme is a very hard task nowadays. However, it seems that some effective three-body Hamiltonian can be defined for the three-body system in the Pauli-allowed subspace [in much the same way as the two-body one from Eq. (32)], so that the diagonalization technique might be generalized for a proper account of three-body correlations as well. Such an approach will simplify enormously the evaluation of three-body force contribution in a traditional scheme.

V. SUMMARY

In the present work, we have demonstrated that the accurate multienergy solution for the Lippmann-Schwinger integral equation for the single- and coupled-channel t matrix can be easily found from the direct single diagonalization procedure for the total Hamiltonian matrix in the L_2 basis of the stationary wave packets. This approach was tested carefully for two particular NN interaction models both for a single channel and also coupled-channel transition operators. In all the cases, a very good accuracy of the direct diagonalization procedure as compared to the solution of the respective integral equation was attained. Thus, this approach provides a very efficient way for finding the coupled-channel off-shell t matrix at various energies.

This important feature is especially valuable for solving the few-body scattering problems where the kernel of the Faddeev-like equation includes the fully off-shell t matrix at many energies.

At the next step, we have generalized this approach to a solution of the Bethe-Goldstone integral equation and derived an explicit form of the effective Hamiltonian in the Pauli-allowed two-particle subspace. Thus, the multiple numerical solutions for the Bethe-Goldstone integral equation for the reaction matrix at different values of the relative momentum and energy have been replaced by a single matrix diagonalization of the effective Hamiltonian in the Pauli-allowed subspace which is much simpler and faster.

The method can be extended to modern modifications of the BHF approach which include more complicated forms of the particle and hole propagators (such as the $pphh$ propagator [5]), nonzero temperature regime, etc. Moreover, this direct diagonalization technique might open a door to reliable and accurate treatment of three- and few-body correlations in dense nuclear matter.

ACKNOWLEDGMENT

The authors appreciate the partial financial support of DFG Grant No. MU 705/10-1, joint DFG-RFBR Grant No. 16-52-12005, and RFBR Grant No. 16-02-00049.

APPENDIX: EIGENVALUES OF THE COUPLED-CHANNEL TOTAL RESOLVENT IN THE WPCD APPROACH

1. Approximation for the total resolvent in a single-channel case

To find the eigenvalues for the total resolvent in the pseudostate basis, let us remind some results from the general WPCD approach [8].

The scattering wave packets for some Hamiltonian $\hat{h}$ are constructed as integrals of the exact scattering wave functions $|\psi(E)\rangle$ over some discretization intervals $[\varepsilon_{i-1},\varepsilon_i]_{i=1}^N$, (similarly to free WPs):

$$|\bar{z}_i\rangle = \frac{1}{\sqrt{\Delta_i}} \int_{\varepsilon_{i-1}}^{\varepsilon_i} dE|\psi(E)\rangle, \quad \Delta_i = \varepsilon_i - \varepsilon_{i-1}. \tag{A1}$$

These scattering WP states, jointly with the possible bound states $|z_n^b\rangle$ of the Hamiltonian, form a WP space for the Hamiltonian $\hat{h}$ with the projector [8]:

$$\mathfrak{p} = \sum_{n=1}^{N_b} |z_n^b\rangle\langle z_n^b| + \sum_{i=1}^{N} |\bar{z}_i\rangle\langle\bar{z}_i|, \tag{A2}$$

where N_b is a number of bound states. The Hamiltonian can be approximated as a finite sum in such a WP space:

$$\hat{h} \approx \mathfrak{p}\hat{h}\mathfrak{p} = \sum_{n=1}^{N_b} |z_n^b\rangle\varepsilon_n^b\langle z_n^b| + \sum_{i=1}^{N} |\bar{z}_i\rangle\bar{\varepsilon}_i\langle\bar{z}_i|, \tag{A3}$$

where ε_n^b and the midpoints $\bar{\varepsilon}_i = \frac{1}{2}[\varepsilon_{i-1} + \varepsilon_i]$ represent eigenvalues of the total Hamiltonian for its bound states and discretized continuum states correspondingly. Then, the finite-dimensional approximation for the total resolvent in the basis built takes the same diagonal form:

$$\hat{g}(E) \approx \mathfrak{p}\hat{g}(E)\mathfrak{p} = \sum_{n=1}^{N_b} \frac{|z_n^b\rangle\langle z_n^b|}{E - \varepsilon_n^b} + \sum_{i=1}^{N} |\bar{z}_i\rangle g_i(E)\langle\bar{z}_i|, \tag{A4}$$

where eigenvalues $g_i(E)$ are expressed as follows [8]:

$$g_i(E) = \frac{1}{\Delta_i}\left[\ln\left|\frac{E - \varepsilon_{i-1}}{E - \varepsilon_i}\right| - i\pi\theta(E \in [\varepsilon_{i-1},\varepsilon_i])\right]. \tag{A5}$$

Here the generalized Heaviside-type theta function is introduced:

$$\theta(E \in [\varepsilon_{i-1},\varepsilon_i]) = \begin{cases} 1, & E \in [\varepsilon_{i-1},\varepsilon_i], \\ 0, & E \notin [\varepsilon_{i-1},\varepsilon_i]. \end{cases} \tag{A6}$$

It should be stressed that the formula (A5) is universal for any Hamiltonian for which the WP states can be constructed. Thus, it is also valid for a free resolvent $g_0(E)$ eigenvalue in the free WP basis (8).

The diagonalization procedure for the total Hamiltonian matrix h in free WP basis $\{|x_i\rangle\}_{i=1}^N$ results in a finite set of eigenvectors $\{|z_i\rangle\}_{i=1}^N$ with the respective eigenenergies $\{E_i\}$. Assume further that these eigenfunctions are enumerated in order of increasing the eigenvalues. If there is a bound state

in the system, the first state $|z_1\rangle$ with negative energy E_1 is assumed to be an approximation for this bound state wave function $|z_b\rangle$, while all the other eigenfunctions with positive eiegenvalues are pseudostates representing somehow the total Hamiltonian continuum. It was shown previously [8] that these normalized pseudostates can be considered as approximations for scattering WPs (rather than approximations for non-normalized scattering wave functions). So one can replace exact scattering WP functions in Eq. (A4) with corresponding pseudostates. Finally, the pseudostate approximation (6) for the total resolvent is found in which the exact eigenvalues (A5) for scattering WPs are used.

The only problem which arises here is how to construct the discretization mesh $\{\varepsilon_i\}$ in such a way that pseudostate energies $\{E_i\}$ are coincided with eigenvalues $\bar{\varepsilon}_i$ from Eq. (A3) in the exact scattering WP basis. Such a reconstruction of the intervals $[\varepsilon_{i-1},\varepsilon_i]_{i=1}^{N}$ can be done approximately by the following way:

$$\varepsilon_0 = 0, \quad \varepsilon_i = \frac{1}{2}[E_i + E_{i+1}], \quad i = 1,\ldots,N-1,$$
$$\varepsilon_N = E_N + \frac{1}{2}(\varepsilon_{N-1} - \varepsilon_{N-2}). \tag{A7}$$

Here the midpoints $\bar{\varepsilon}_i$ of the reconstructed bins differ a little bit from the exact E_i values, however, with increasing the basis dimension, this difference becomes smaller and does not cause visible errors in the whole solution.

Thus, the eigenvalues of the total resolvent in the pseudostate basis can be found by using the formula (A5) in which endpoints of the energy intervals are calculated from pseudoenergies E_i using Eq. (A7).

2. Coupled-channel pseudostates and the total resolvent eigenvalues

In case of the coupled-channel total Hamiltonian $\hat{h}$, the scattering wave packets are constructed from the exact scattering wave functions $|\psi^{\varkappa}(E)\rangle$ defined in the eigenchannel representation. So, for this purpose, the continuous spectra in eigenchannels $\varkappa$=1 and 2 are divided onto intervals $\{[\varepsilon_{k-1}^{\varkappa},\varepsilon_k^{\varkappa}]_{k=1}^{N_{\varkappa}}\}_{\varkappa=1}^{2}$ and the coupled-channel scattering WPs are introduced:

$$|\bar{z}_k^{\varkappa}\rangle = \frac{1}{\sqrt{\Delta_k^{\varkappa}}}\int_{\varepsilon_{k-1}^{\varkappa}}^{\varepsilon_k^{\varkappa}} dE|\psi^{\varkappa}(E)\rangle, \quad \Delta_k^{\varkappa} = \varepsilon_k^{\varkappa} - \varepsilon_{k-1}^{\varkappa}, \tag{A8}$$

similarly to the one-channel case.

Further, one adds the possible bound states and introduces the WP space for the total coupled-channel Hamiltonian, similarly to the one-channel case. At last, one gets the following WP approximation for the total coupled-channel resolvent,

$$\hat{g}(E) \approx \sum_{n=1}^{N_b}\frac{|z_n^b\rangle\langle z_n^b|}{E-E_n} + \sum_{\varkappa=1}^{2}\sum_{k=1}^{N_{\varkappa}}|\bar{z}_k^{\varkappa}\rangle g_k^{\varkappa}(E)\langle\bar{z}_k^{\varkappa}|, \tag{A9}$$

where eigenvalues $g_k^{\varkappa}(E)$ are defined by the formula:

$$g_k^{\varkappa}(E) = \frac{1}{\Delta_k^{\varkappa}}\left[\ln\left|\frac{E-\varepsilon_{k-1}^{\varkappa}}{E-\varepsilon_k^{\varkappa}}\right| - i\pi\theta\left(E\in\left[\varepsilon_{k-1}^{\varkappa},\varepsilon_k^{\varkappa}\right]\right)\right], \tag{A10}$$

which is just the same as Eq. (A5) for the single-channel resolvent eigenvalues where the $\varkappa$-channel interval endpoints $\varepsilon_k^{\varkappa}$ should be used.

To treat coupled-channel pseudostates, we have shown previously [8,14] that the free WP basis states in the initial unperturbed channels (e.g., channels corresponding to the fixed orbital momentum l value) should be constructed in such a way that the free Hamiltonian matrix has degenerate discrete eigenvalues [8,14]. In such a case, the spectrum of the total Hamiltonian matrix **h** consists of pairs of slightly shifted nearby eigenenergies (except possible bound states). Thus, this spectrum can be separated onto two branches. Finally, these two separated branches of eigenvalues are considered as discretized eigenchannel spectra.

For the two-channel case discussed in the present paper, this separation is done just by dividing the eigenvalues of the total Hamiltonian matrix with even and odd indices. Further, the discretization endpoints are built for each of two eigenchannels $\varkappa = 1,2$ separately from the eigenvalues $E_i^{\varkappa}$ by using the algorithm similar to the single-channel one (A7).

[1] R. G. Newton, *Scattering Theory of Waves and Particles* (McGraw-Hill, New York, 1966).
[2] M. I. Haftel and F. Tabakin, Nucl. Phys. A **158**, 1 (1970).
[3] E. Schiller, H. Müther, and P. Czerski, Phys. Rev. C **59**, 2934 (1999).
[4] M. Baldo, A. Fiasconaro, H. Q. Song, G. Giansiracusa, and U. Lombardo, Phys. Rev. C **65**, 017303 (2001).
[5] W. H. Dickhoff and D. van Neck, *Many-Body Theory Exposed! Propagator Description of Quantum Mechanics in Many-body Systems* (World Scientific, Singapore, 2005).
[6] T. Frick, Kh. Gad, H. Müther, and P. Czerski, Phys. Rev. C **65**, 034321 (2002).
[7] R. Sartor, Phys. Rev. C **73**, 034307 (2006).
[8] O. A. Rubtsova, V. I. Kukulin, and V. N. Pomerantsev, Ann. Phys. **360**, 613 (2015).
[9] E. J. Heller, T. N. Rescigno, and W. P. Reinhardt, Phys. Rev. A **8**, 2946 (1973).
[10] J. R. Winick and W. P. Reinhardt, Phys. Rev. A **18**, 910 (1978); **18**, 925 (1978).
[11] Z. Papp, C-.Y. Hu, Z. T. Hlousek, B. Kónya, and S. L. Yakovlev, Phys. Rev. A **63**, 062721 (2001).
[12] S. Quaglioni, W. Leidemann, G. Orlandini, N. Barnea, and V. D. Efros, Phys. Rev. C **69**, 044002 (2004).
[13] D. Ding, A. Rios, H. Dussan, W. H. Dickhoff, S. J. Witte, and A. Polls, arXiv:1601.01600.
[14] O. A. Rubtsova, V. I. Kukulin, V. N. Pomerantsev, and A. Faessler, Phys. Rev. C **81**, 064003 (2010).
[15] O. A. Rubtsova, V. I. Kukulin, and V. N. Pomerantsev, Phys. Rev. C **84**, 044002 (2011).
[16] M. Baldo, I. Bombaci, L. S. Ferreira, G. Giansiracusa, and U. Lombardo, Phys. Rev. C **43**, 2605 (1991).

[17] M. Danos and W. Greiner, Phys. Rev. **146**, 708 (1966).
[18] R. Machleidt, F. Sammarruca, and Y. Song, Phys. Rev. C **53**, R1483 (1996).
[19] V. G. J. Stoks, R. A. M. Klomp, C. P. F. Terheggen, and J. J de Swart, Phys. Rev. C **49**, 2950 (1994).
[20] H. A. Bethe, B. H. Brandow, and A. G. Petchek, Phys. Rev. **129**, 225 (1963).
[21] H. Q. Song, M. Baldo, G. Giansiracusa, and U. Lombardo, Phys. Rev. Lett. **81**, 1584 (1998).
[22] J. P. Jeukenne, A. Lejeune, and C. Mahaux, Phys. Rev. C **16**, 80 (1977).
[23] F. Isaule, H. F. Arellano, and A. Rios, arXiv:1602.05234.
[24] A. B. Migdal, *Theory of Finite Fermi Systems* (Wiley, New York, 1967).
[25] J. R. Schrieffer, *Theory of Superconductivity* (Benjamin, Amherst, 1964).
[26] G. D. Mahan, *Many-Particle Physics* (Plenum Press, New York 1981).
[27] T. Frick and H. Müther, Phys. Rev. C **68**, 034310 (2003).
[28] H. Müther and W. H. Dickhoff, Phys. Rev. C **72**, 054313 (2005).
[29] C. Mahaux and R. Sartor, in *Advances in Nuclear Physics*, edited by J. W. Negele and E. Vogt (Premium press, New York-London, 1991), Vol. 20, p. 1.
[30] Kh. Gad, Nucl. Phys. A **747**, 655 (2005).